Journal of Food and Drug Analysis

Volume 29 | Issue 2 Article 6

2021

# Ursolic acid restores sensitivity to gemcitabine through the RAGE/NF-ĸB/MDR1 axis in pancreatic cancer cells and in a mouse xenograft model

ORIGINAL ARTICLE

# Ursolic acid restores sensitivity to gemcitabine through the RAGE/NF-κB/MDR1 axis in pancreatic cancer cells and in a mouse xenograft model

Zih-Ying Li[1], Sheng-Yi Chen[1], Ming-Hong Weng, Gow-Chin Yen*

Department of Food Science and Biotechnology, National Chung Hsing University, 145 Xingda Road, Taichung, 40227, Taiwan

**Abstract**

**Gemcitabine (GEM) is a first-line drug for pancreatic cancer therapy, but GEM resistance is easily developed in patients. Growing evidence suggests that cancer chemoprevention and suppression are highly associated with dietary phytochemical and microbiota composition. Ursolic acid (UA) has anti-inflammatory and anticancer effects; however, its role in improving cancer drug resistance *in vivo* remains unclear. In this study, the aim was to explore the role of UA in managing drug resistance-associated molecular mechanisms and the influence of gut microbiota. The *in vitro* results showed that receptor for advanced glycation end products (RAGE), nuclear factor kappa B p65 (NF-κB/p65), and multidrug resistance protein 1 (MDR1) protein levels were significantly increased in GEM-resistant pancreatic cancer cells (named MIA PaCa-2 $^{GEMR}$) compared to MIA PaCa-2 cells. Downregulation of RAGE, pP65, and MDR1 protein expression not only was observed following UA treatment but also was seen in MIA PaCa-2 $^{GEMR}$ cells after transfection with a RAGE siRNA. Remarkably, the enhanced effects of UA coupled with GEM administration dramatically suppressed the RAGE/NF-κB/MDR1 cascade and consequently inhibited subcutaneous tumor growth. Moreover, UA could increase alpha diversity and regulate the composition of gut microbiota, especially in *Ruminiclostridium 6*. Taken together, these results provide the first direct evidence of MDR1 attenuation and chemosensitivity enhancement through inhibition of the RAGE/NF-κB signaling pathway *in vitro* and *in vivo*, implying that UA may be used as an adjuvant for the treatment of pancreatic cancer in the future.**

*Keywords:* Ursolic acid, Chemosensitivity, Pancreatic cancer, MDR1, Microbiota

## 1. Introduction

Pancreatic cancer is the most aggressive and lethal cancer due to a lack of standard screening guidelines for patients at the early asymptomatic stage [1, 2]. There are numerous treatment options for pancreatic cancer, such as surgical resection, neoadjuvant therapy, chemotherapy, radiation therapy, targeted therapy, and immunotherapy [3]. Nevertheless, severe side effects, complications, and drug resistance are observed and considered an important part of cancer care [4]. In the absence of effective and safe therapeutic strategies, perhaps the incidence and mortality of pancreatic cancer will escalate and become the second leading cause of cancer-related death by 2030 [5]. Thus, there is a strong need for additional prevention and treatment tools for pancreatic cancer.

Ursolic acid (UA) is a natural pentacyclic triterpene compound that is widely found in *Hedyotis diffusa*, *Prunella vulgaris*, *Rosmarinus officinalis*, coffee, and fruit peels, particularly in apple peels [6]. Several studies have revealed the anticancer properties of UA, including restraint of cancer progression through cell proliferation inhibition, motility suppression, tumor microenvironment modulation,

*Abbreviations:* **GEM**, gemcitabine; **MDR1**, multidrug resistance protein 1; **NF-κB/p65**, nuclear factor kappa B p65; **RAGE**, receptor for advanced glycation end products; **siRNA**, small interfering RNA; **UA**, ursolic acid.

Received 12 January 2021; accepted 16 March 2021.
Available online 15 June 2021.

* Corresponding author: Tel: 886-4-2287-9755; Fax: 886-4-2285-4378.
E-mail address: gcyen@nchu.edu.tw (G.-C. Yen).
[1] These authors contributed equally to this work.

https://doi.org/10.38212/2224-6614.3346

and cell death induction [7-11]. Moreover, no toxicological effects were observed in a 90-day oral toxicity study in male and female rats receiving up to 1000 mg/kg/daily UA via oral gavage [12]. This evidence indicates the safety of UA in cancer prevention and treatment.

To date, drug resistance is the major problem in pancreatic cancer therapy and is one of the main challenges for the extremely poor prognosis of pancreatic cancer [13]. Gemcitabine (GEM) is a cytidine analog that is the standard drug for pancreatic cancer chemotherapy and acts as a competitive substrate of deoxycytidine triphosphate (dCTP) to block cell cycle progression and DNA synthesis [14]. However, the intrinsic and environment-mediated drug resistance of GEM frequently leads to treatment failure as well as recurrence in patients after potentially curative resection [15]. Thus, targeting GEM efflux could be an effective strategy for pancreatic cancer treatment.

The receptor for advanced glycation end products (RAGE) is a transmembrane and multi-ligand component of the immunoglobulin superfamily, which has been shown to promote pancreatic tumorigenesis by leading to the activation of multiple downstream signaling cascades [16]. Moreover, numerous studies have demonstrated that a positive feedback loop between RAGE and NF-κB is found and results in maintaining RAGE activation and proliferation signaling in pancreatic cancer [17, 18]. However, little is known about the role of RAGE in the chemoresistance of pancreatic cancer. Besides, accumulating evidence has revealed that multidrug resistance protein 1 (MDR1) plays a crucial role in GEM efflux and consequently increases GEM resistance ability in cancers [19, 20]. The study provided compelling evidence that RAGE-initiated ERK/Drp1 signaling triggers chemoresistance and regrowth in dying colorectal cancer cells [21]. In line with this, our recent results demonstrated that RAGE upregulation promotes the development of GEM-resistant cells and is abolished by quercetin treatment [22].

The gut microbiota has been shown to be highly associated with pancreatic health and disease, but clarification of the detailed mechanisms contributing to the pathologies have been slow to emerge [23]. Recently, studies revealed that the gut microbiome promotes pancreatic cancer progression and tumor-immune escape mechanisms via decreasing monocyte differentiation, which consequently causes T-cell anergy [24]. Hence, targeting the microbiome may protect against tumorigenesis.

Until now, the capacity of UA to regulate GEM resistance-associated mechanisms and the microbiome is still unclear. Therefore, exploring the role of UA in modulating both MDR1 expression through the RAGE/NF-κB axis and microbiota dysbiosis may provide a benefit to pancreatic cancer treatment.

## 2. Materials and methods

### 2.1. Chemicals and reagents

UA, GEM, sodium bicarbonate, penicillin-streptomycin (PS), sodium dodecyl sulfate (SDS), glycine, trishydroxymethylaminomethane (Tris), isopropanol, Tween 20, bovine serum albumin (BSA), and other chemicals were of analytical grade and were obtained from Sigma-Aldrich (St. Louis, MO, USA). High-glucose DMEM, Opti-MEM, horse serum, and fetal bovine serum were obtained from Gibco/Life Technologies (Carlsbad, CA, USA). A MDR1 antibody (for *in vivo* experiments), as well as RAGE and NF-κB/p65 antibodies were purchased from Abcam (Cambridge, MA, USA). Phospho-NF-κB/p65 (Ser 536; sc-101752) and phospho-IκB-α (Ser 32/36; sc-101713) antibodies were purchased from Santa Cruz (Santa Cruz, CA). MDR1 antibody (for *in vitro* experiments) was obtained from Cell Signaling Technology (Beverly, MA, USA). β-actin (AC-15) antibody was purchased from Novus Biologicals (Littleton, CO, USA). Peroxidase AffiniPure goat anti-mouse IgG (H + L) and peroxidase AffiniPure goat anti-rabbit IgG (H + L) were purchased from GeneTex (Irving, CA, USA). A RAGE siRNA and Dharmacon transfection reagent were purchased from GE Healthcare (Lafayette, CO, USA).

### 2.2. Cell culture

The human pancreatic carcinoma cell line MIA PaCa-2 was obtained from the Bioresource Collection and Research Center (BCRC; Hsinchu, Taiwan). The cells were cultured in high glucose DMEM supplemented with 10% v/v fetal bovine serum, 2.5% v/v horse serum, 1.5 g/L sodium bicarbonate, and 1% penicillin-streptomycin. A GEM-resistant cell line (MIA PaCa-2 $^{GEMR}$ cells) was established by incrementally increasing GEM concentrations (from 0.05 μM to 0.5 μM) in culture medium for developing a cellular model that tolerated 0.5 μM GEM [22]. Cells were maintained at 37°C in a humidified incubator with 5% v/v $CO_2$ and 95% v/v air.

### 2.3. Cell viability analysis

Cells were placed into 96-well microtiter plates overnight and then were treated with different concentrations of UA or GEM. After treatments, an MTT assay was performed as described in our

previous report [22], and the optical densit (OD) at 570 nm was measured by a FLUOstar Galaxy spectrophotometer (BMG LABTECH, Ortenberg, Germany). Cell viability is presented as a percentage relative to the control.

### 2.4. Xenograft tumor model

Four-week-old female BALB/c nude mice were purchased from the National Laboratory Animal Center (Taipei, Taiwan) and were kept in specific pathogen-free (SPF) conditions. All mice had ad libitum access to a chow diet (LabDiet 5001 Rodent Diet; Newco Distributors Corporation, Rancho Cucamonga, CA, USA) and distilled water. The mice were kept in a regular environment with the following conditions: light-dark cycle (12:12 h), humidity (65% ± 5%), and room temperature (22°C ± 2°C). All mice were given one week to accommodate the environment and diet. The protocols of animal experiments were approved by the Institutional Animal Care and Use Committee (IACUC) of National Chung Hsing University (IACUC Approval no: 106-107$^{R}$).

In this study, the beneficial effects of UA on chemosensitivity enhancement were evaluated in a GEM-resistant pancreatic cancer xenograft mouse model. MIA PaCa-2 $^{GEMR}$ cells were resuspended at a final concentration of $3 \times 10^6$ cells per 100 μL of serum-free DMEM culture medium mixed with Matrigel (1:1), and then they were injected subcutaneously into the right flank of the nude mice. When tumors reached 100 mm$^3$ in volume, the mice were randomly divided into four groups (8 animals each group) and were injected intraperitoneally (IP) with normal saline (untreated control group), GEM (100 mg/kg b.w.), UA (40 mg/kg b.w.), and GEM (100 mg/kg b.w.) combined with UA (40 mg/kg b.w.) 8 times (once every three days). The dose for GEM treatment was based on previous reports [25, 26]. Additionally, the tumor suppression effects were useful by UA treatment in the range of 50–200 mg/kg/d [27, 28]. In our pretest condition, 40 mg/kg UA (IP injection, once every three days) effectively reduced tumor growth (data not shown). Thus, the 40 mg/kg UA was selected for use in this study. All treatments were performed by IP injection into the abdominal cavity once every three days. The mice were then monitored for tumor progression with a caliper every other day. Tumor size was measured across its two perpendicular diameters, and its volume was calculated as 1/2 (length × width$^2$). Blood samples were collected for GOT, GPT, BUN, and creatinine analysis by Union Clinical Laboratory (Taichung, Taiwan).

### 2.5. Small interfering RNA knockdown

The siRNA transfection procedure was carried out following the manufacturer's instructions. Briefly, 25 nM RAGE siRAGE or 25 nM vehicle vector control reagent was prepared, mixed with Opti-MEM and incubated at room temperature for 20 minutes. To perform the siRNA transfection, cells were incubated with the above reagents for 24 h, and then the RAGE protein levels were checked.

### 2.6. Protein expression analysis

After *in vitro* or *in vivo* experiments, the cell lysates or tumor tissue homogenates were harvested, and protein concentrations were determined. The expression levels of RAGE, NF-κB/p65, phospho-IκB-α, and MDR1 in the cells and tissues were determined using Western blotting analysis, according to our previous report [22]. The relative abundances of the signal intensities were quantified using VisionWorks LS Image Acquisition and Analysis Software (version 6.3.3, UVP, Upland, CA, USA).

### 2.7. Gut microbiota analysis

Mouse fecal specimens were collected and immediately frozen at −80°C until DNA extraction was performed. DNA was extracted using an AllPure Genomic DNA Extraction Kit (Allbio, Taichung, Taiwan) according to the manufacturer's instructions. After extraction, the total DNA concentration was quantified using a Qubit 2.0 Fluorometer (Invitrogen, Carlsbad, CA, USA). The V3 and V4 hypervariable regions of prokaryotic 16S ribosomal DNA were selected for generating amplicons and the following taxonomy analysis. For amplification of the V3–V4 region of 16S rDNA, forward primer (5′-CCTACGGRRBGCASCAGKVRVGAAT-3′) and reverse primer (5′- GGACTACNVGGGTWTC-TAATCC-3′) were used. The bioinformatics analysis of microbial diversity studies was performed by Allbio Life Co., Ltd. (Taichung, Taiwan).

### 2.8. Statistical analysis

All data are presented as the mean ± SD and were analyzed using SPSS statistical software. Differences between groups were analyzed by one-way analysis of variance (ANOVA) or Student's t-test. Statistical significance was assumed and defined at a $p$-value $< 0.05$.

## 3. Results

### 3.1. Comparison of chemoresistance-associated protein expression in MIA PaCa-2 and MIA PaCa-2 $^{GEMR}$ cells

As shown in Fig. 1A and B, tolerance to GEM pharmacologic cytotoxicity was greater in MIA PaCa-2 $^{GEMR}$ cells than it was parental cells. The half-maximal inhibitory concentration ($IC_{50}$) value of GEM treatment in MIA PaCa-2 cells was 0.064 ± 0.017 μM, whereas the $IC_{50}$ value was 54.4 ± 5.12 μM in GEM-resistant cells; this was approximately 850-fold higher than the value in the parental cells. Recently, we demonstrated that RAGE activation contributes to GEM resistance in pancreatic cancer [22]. Thus, we further hypothesized that RAGE-initiated signaling might promote MDR1 levels in MIA PaCa-2 $^{GEMR}$ cells. Consistent with this possibility, RAGE protein levels were significantly increased in GEM-resistant cells compared to MIA PaCa-2 cells (Fig. 1C). Growing evidence suggests that the NF-κB signaling pathway and its associated genes play a central role in GEM resistance in pancreatic cancer [29], indicating that MDR1 protein expression may be modulated by NF-κB signaling. As anticipated, the protein levels of pIκB-α (Ser 32/36), NF-κB pP65 (Ser 536), and MDR1 were increased in GEM-resistant pancreatic cancer cells (Fig. 1D and E).

### 3.2. UA inhibited cell viability and chemoresistance-associated protein expression in MIA PaCa-2 $^{GEMR}$ cells

Our previous studies have found that UA induces cell death in various cancer cell lines through

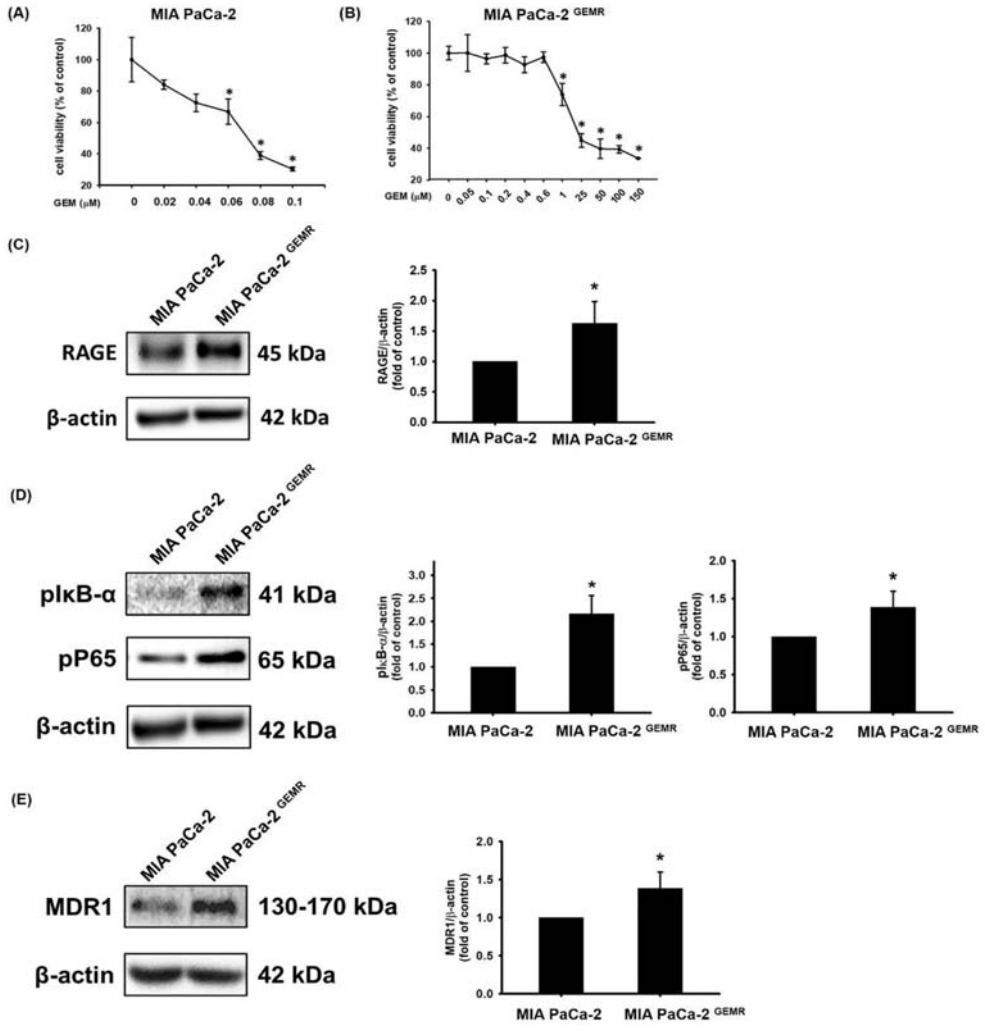


*Fig. 1. Upregulation of RAGE and MDR1 in GEM-resistant MIA PaCa-2 cells. Cells were treated with GEM for 72 h, and then the cell viability of (A) MIA PaCa-2 and (B) MIA PaCa-2 $^{GEMR}$ cells was evaluated by MTT assay. Protein levels of (C) RAGE, (D) pIκB-α and pP65, and (E) MDR1 were analyzed by Western blotting. Protein quantification shows the mean ± SD of three independent measurements. In (A) and (B), asterisks indicate $p < 0.05$ vs. untreated cells. In (C), (D), and (E), asterisks represent $p < 0.05$ vs. MIA PaCa-2 cells.*

distinct mechanisms [30-33]. Here, we investigated whether UA has the same lethal capacity in pancreatic-resistant cancer cells. The cell viability was not merely repressed by UA treatment in GEM-sensitive cells; viability was significantly reduced in MIA PaCa-2 $^{GEMR}$ cells in a dose-response manner as well (Fig. 2A and B). To elucidate the molecular mechanisms of chemosensitivity enhancement by

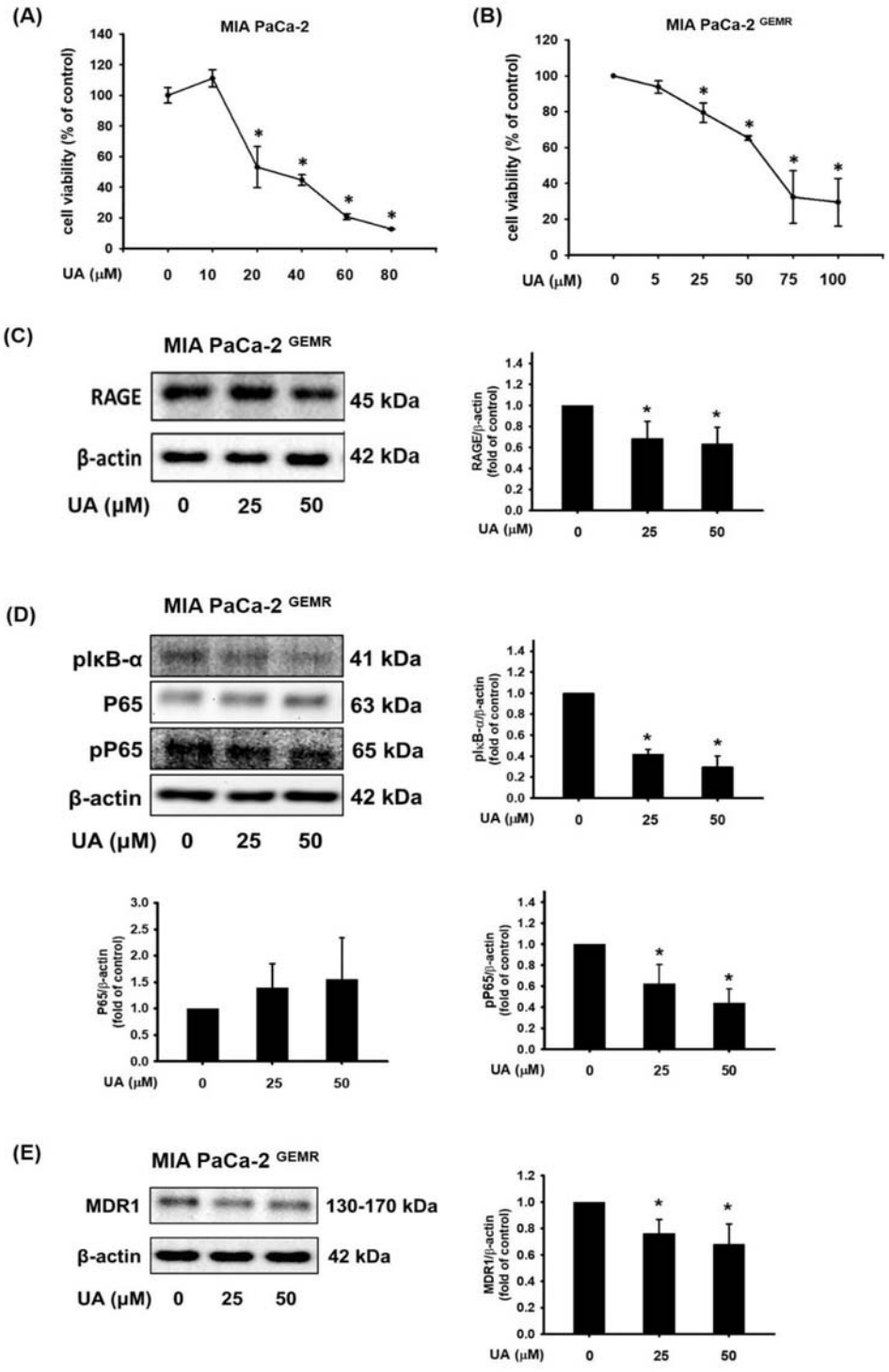


*Fig. 2. UA reduced cell growth and RAGE/NFκB/MDR1 protein expression. The viability of (A) MIA PaCa-2 and (B) MIA PaCa-2 $^{GEMR}$ cells was evaluated by MTT assay. Cells were treated with UA for 24 h, and the protein expression levels of (C) RAGE, (D) pIκB-α and pP65, and (E) MDR1 were analyzed by Western blotting. Protein quantification shows the mean ± SD of three independent measurements. *$p < 0.05$ vs. untreated cells.*

UA treatment, we examined the associated protein expression in GEM-resistant cells. The levels of RAGE were downregulated in MIA PaCa-2 $^{GEMR}$ cells subjected to various concentrations of UA (Fig. 2C). Moreover, the phosphorylation activity of IκB-α (Ser 32/36) and NF-κB P65 (Ser 536) was significantly suppressed by UA treatment (Fig. 2D). In addition, UA incubation effectively inhibited MDR1 levels in GEM-resistant cells (Fig. 2E).

### *3.3. RAGE regulated MDR1 expression in MIA PaCa-2 $^{GEMR}$ cells*

To determine whether IκB-α, NF-κB, and MDR1 protein expression was directly controlled via RAGE regulation in MIA PaCa-2 $^{GEMR}$ cells. MIA PaCa-2 $^{GEMR}$ cells were transfected with an empty vector (denoted Vehicle cells) or a RAGE siRAGE (denoted siRAGE cells) and examined for pIκB-α, NF-κB pP65, and MDR1 protein levels by Western blotting. RAGE silencing greatly decreased IκB-α (Ser 32/36) and NF-κB P65 (Ser 536) protein phosphorylation and consequently abolished MDR1 protein expression compared with what was observed in control cells (Fig. 3).

### *3.4. Chemosensitivity was enhanced by UA treatment and RAGE gene silencing*

The objective of this study was to determine the chemosensitivity enhancing effects of UA treatment or RAGE siRNA transfection in MIA PaCa-2 $^{GEMR}$ cells. As shown in Fig. 4A and B, the RAGE protein levels were significantly decreased by RAGE siRNA transfection compared to the vehicle cells. Likewise, the protein expression of RAGE was also reduced by UA incubation compared to the vehicle cells (Fig. 4A and B). Furthermore, UA treatment or RAGE siRNA transfection dramatically decreased GEM-evoked RAGE expression contrast to that of the GEM-treated vehicle cells (Fig. 4A and B). Also, the trends of NF-κB P65 (Ser 536) protein phosphorylation and MDR1 levels were similar to the RAGE protein expression in the various treatment groups (Fig. 4C and D). Notably, UA treatment or RAGE gene silencing effectively diminished MDR1 protein expression under GEM treatment conditions (Fig. 4D).

### *3.5. GEM chemosensitivity was enhanced by UA administration in MIA PaCa-2 $^{GEMR}$-bearing xenograft mice*

It is critical to determine whether GEM resistance was overcome by UA administration *in vivo*. MIA PaCa-2 $^{GEMR}$ cells were injected subcutaneously into nude mice to establish xenografts. The tumor size and nodule volume were not significantly different between the untreated control and GEM-treated groups (Fig. 5A and B). Impaired tumorigenesis was observed in the UA group compared with the untreated control group (Fig. 5A and B). Remarkably,

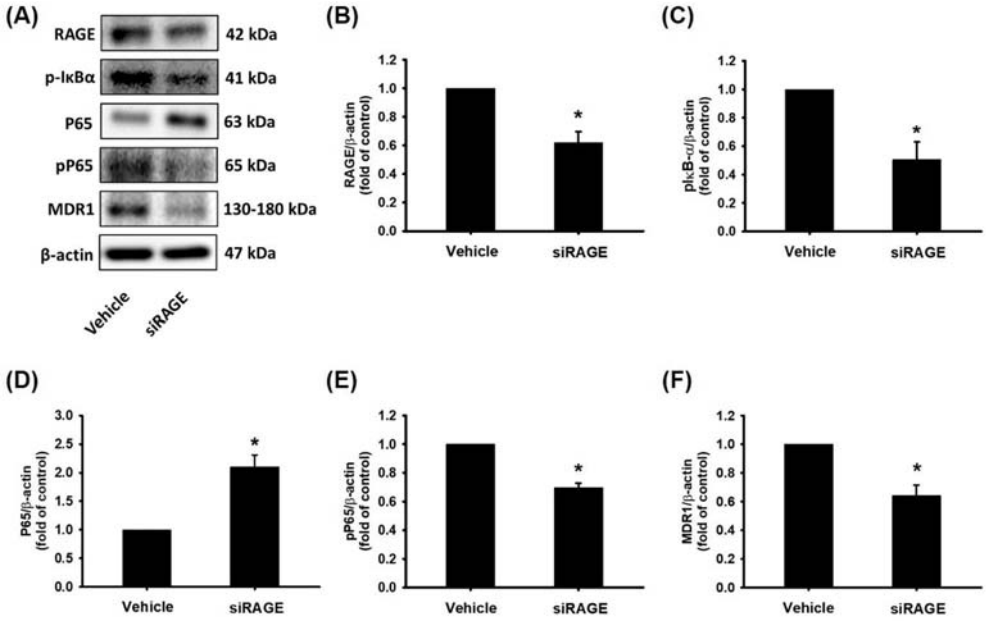


*Fig. 3. Knocking down RAGE gene expression repressed pIκB-α, pP65 and MDR1 protein levels in MIA PaCa-2 $^{GEMR}$ cells. Cells were transfected with an empty vector (named Vehicle cells) or a RAGE siRAGE (named siRAGE cells), and (A) the protein levels of RAGE, pIκB-α, P65, pP65, and MDR1 were analyzed by Western blotting. (B–F) The relative expression levels of RAGE, pIκB-α, P65, pP65, and MDR1 protein are expressed as the mean ± SD of three independent measurements. *$p < 0.05$ vs. vehicle cells.*

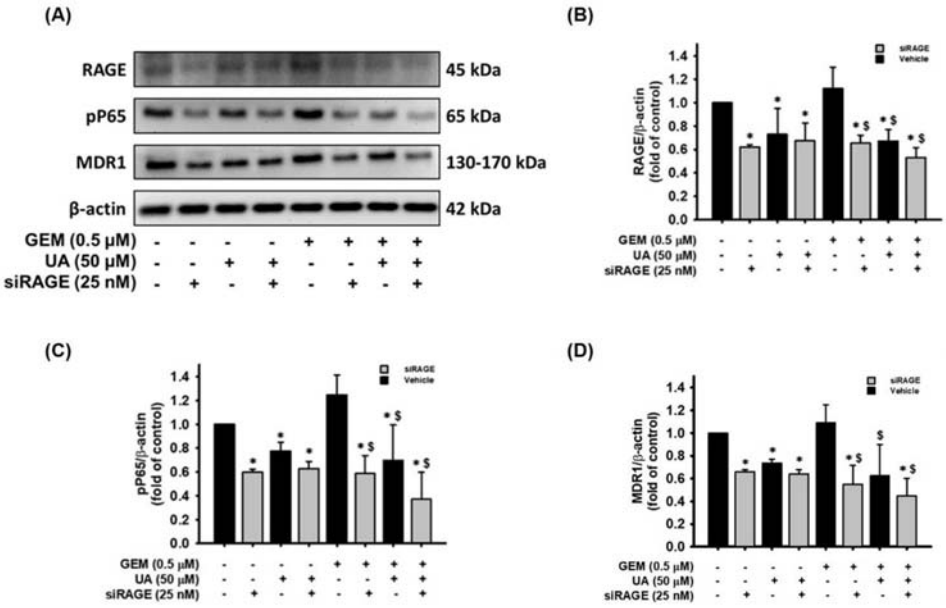


*Fig. 4. Enhancement effect of UA plus RAGE siRNA treatment on RAGE, pP65, and MDR1 protein downregulation. MIA PaCa-2 $^{GEMR}$ cells were transfected with an empty vector (named Vehicle cells) or a RAGE siRAGE (named siRAGE cells). Vehicle cells and siRAGE cells treated with or without 50 μM UA and 0.5 μM GEM for 24 h, respectively. (A) RAGE, pP65, and MDR1 protein expression was analyzed by Western blotting. The relative protein levels of (B) RAGE, (C) pP65, and (D) MDR1 are shown as the mean ± SD of three independent measurements. *p < 0.05 vs. untreated vehicle cells, $^{\$}p < 0.05$ vs. GEM-treated vehicle cells.*

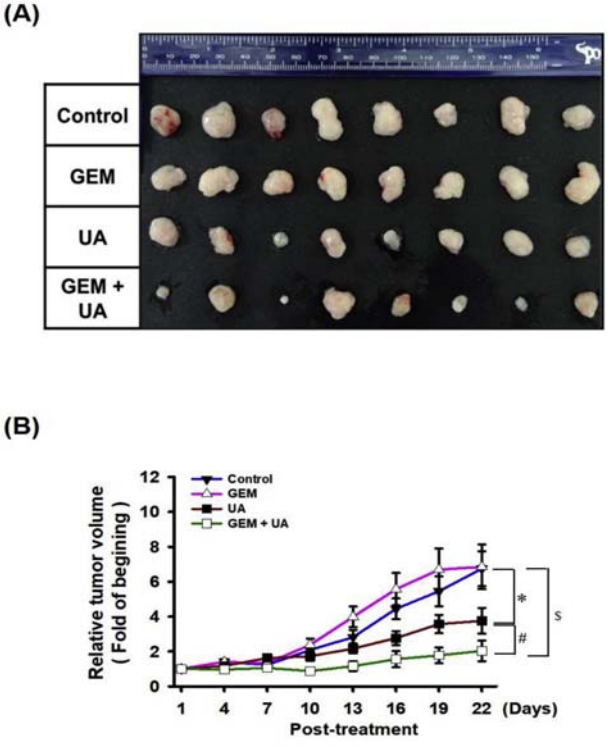


*Fig. 5. Chemosensitivity promoted by UA administration in MIA PaCa-2 $^{GEMR}$-bearing xenograft mice. When tumors reached 100 mm$^3$ in volume, UA and GEM were administered by IP injection into the abdominal cavity 8 times (once every three days). (A) The photographs illustrate representative features of tumor growth after injection. (B) The relative tumor volume was calculated after the initial treatment. Error bars indicate the S.E.M. (n = 8 mice/group). *p < 0.05 vs. Control group; $^{\#}p < 0.05$ vs. UA group; $^{\$}p < 0.05$ vs. GEM group.*

the volume and weight of xenograft tumors were dramatically decreased by GEM plus UA treatment compared to UA or GEM treatment (Fig. 5A and B).

The involvement of the RAGE/NF-κB/MDR1 axis *in vivo* was then further examined. As shown in Fig. 6A, RAGE protein levels were significantly increased in the GEM group compared with the untreated control group. UA or GEM plus UA treatment effectively reduced RAGE protein expression (Fig. 6A). *In vitro* experiments showed that RAGE activation was responsible for NF-κB and MDR1 expression. Further, a similar pattern was also observed for NF-κB P65 and MDR1 protein expression. The phosphorylation of NF-κB P65 (Ser 536) was increased by GEM administration in MIA PaCa-2 $^{GEMR}$ cell-bearing tumors (Fig. 6B). The phosphorylation activities of NF-κB P65 (Ser 536) protein were significantly reduced by UA or GEM plus UA treatment (Fig. 6B). Similar protein expression patterns were not only found regarding RAGE and NF-κB P65 expression, but the same expression tendency was found for MDR1 protein in the xenograft experiment (Fig. 6C).

On the other hand, the safety of UA treatment was evaluated by biochemical analysis of the blood. The examination revealed that serum glutamic oxaloacetic transaminase (GOT), glutamic pyruvic transaminase (GPT), blood urea nitrogen (BUN), and creatinine contents were significantly increased in the GEM treatment group in comparison to the

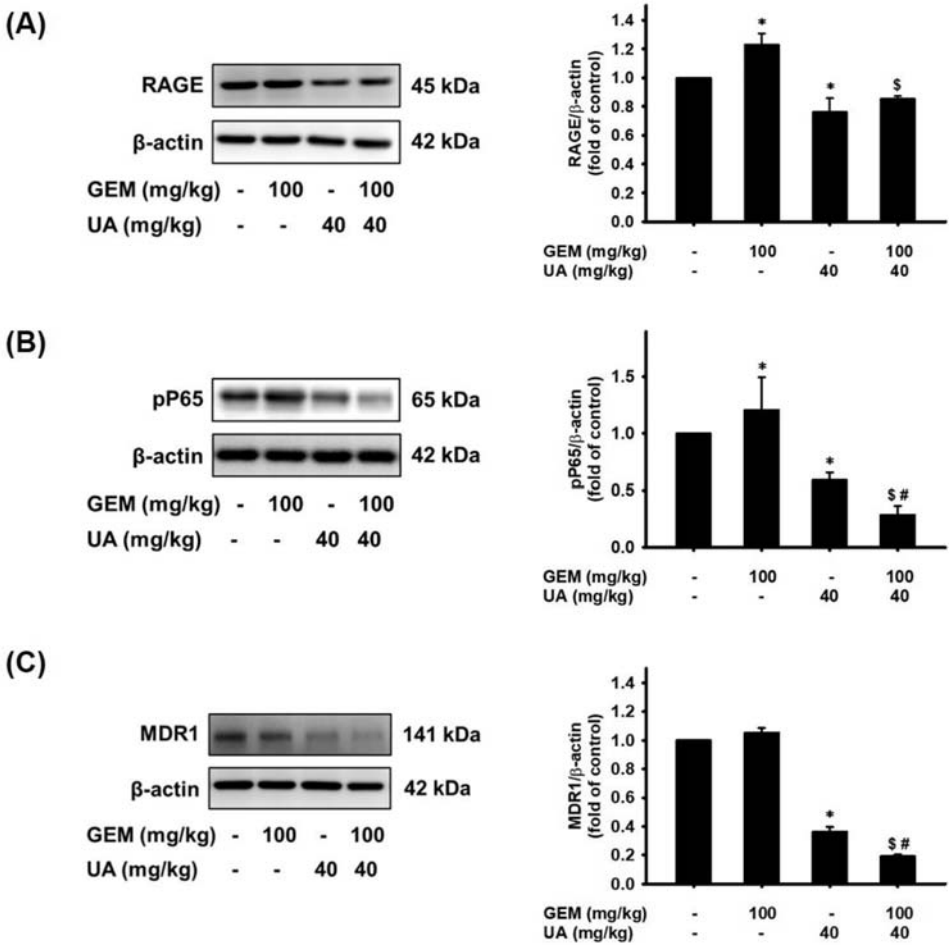


*Fig. 6. Suppression of RAGE, pP65, and MDR1 protein expression by UA administration in vivo. Treatment with GEM coupled with or without UA in MIA PaCa-2 $^{GEMR}$-bearing xenograft mice. Tumor tissues were homogenized for (A) RAGE, (B) pP65, and (C) MDR1 protein analysis. The relative expression of RAGE protein is expressed as the mean ± S.E.M. *$p < 0.05$ vs. Control group, $^{\$}p < 0.05$ vs. GEM group, and $^{\#}p < 0.05$ vs. UA group.*

untreated control group (Fig. 7). Surprisingly, UA plus GEM treatment dramatically reduced GOT, BUN, and creatinine levels compared with those of the GEM-treated group (Fig. 7).

### *3.6. Pancreatic cancer-associated microbiota was modulated by UA administration*

Growing evidence suggests that the gut microbiota is one of multiple sources of influence on oncogenesis and chemotherapy [23, 24]. The richness and species diversity of gut microbiota (α-diversity) were estimated by Chao1 and Shannon indexes. The Chao1 and Shannon indexes were lower in the GEM-treated mice than they were in the other groups (Fig. 8A and B). *Firmicutes* and *Bacteroidetes* were two major phyla in MIA PaCa-2 $^{GEMR}$ cell-bearing xenograft mice. GEM treatment considerably decreased the proportion of *Firmicutes*/*Bacteroidetes*, whereas the proportion was slightly increased by UA or UA plus GEM treatment (Fig. 8C). In addition, the relative abundance of the top 5 most abundant bacterial strains was assessed. Decreasing relative abundances of *Anaeroplasma*, the *Eubacterium xylanophilum* group, and *Roseburia* were observed in the GEM-treated group compared with the untreated control group (Fig. 8D). In contrast, the relative abundances of *Parabacteroides* and *Ruminiclostridium 6* were increased in the GEM group compared with the untreated control group (Fig. 8D). Interestingly, the relative abundance of *Ruminiclostridium 6* was repressed by UA treatment to levels that were lower than those of the untreated control group (Fig. 8E). Moreover, UA plus GEM treatment significantly increased the relative abundance of *Erysipelatoclostridium* and reduced the relative abundance of *Mucispirillum* and *Ruminiclostridium 6* compared with their levels in the GEM-treated mice (Fig. 8F). On the basis of the above results suggested that the relative abundance of *Ruminiclostridium 6* may be directly regulated by UA administration in mice.

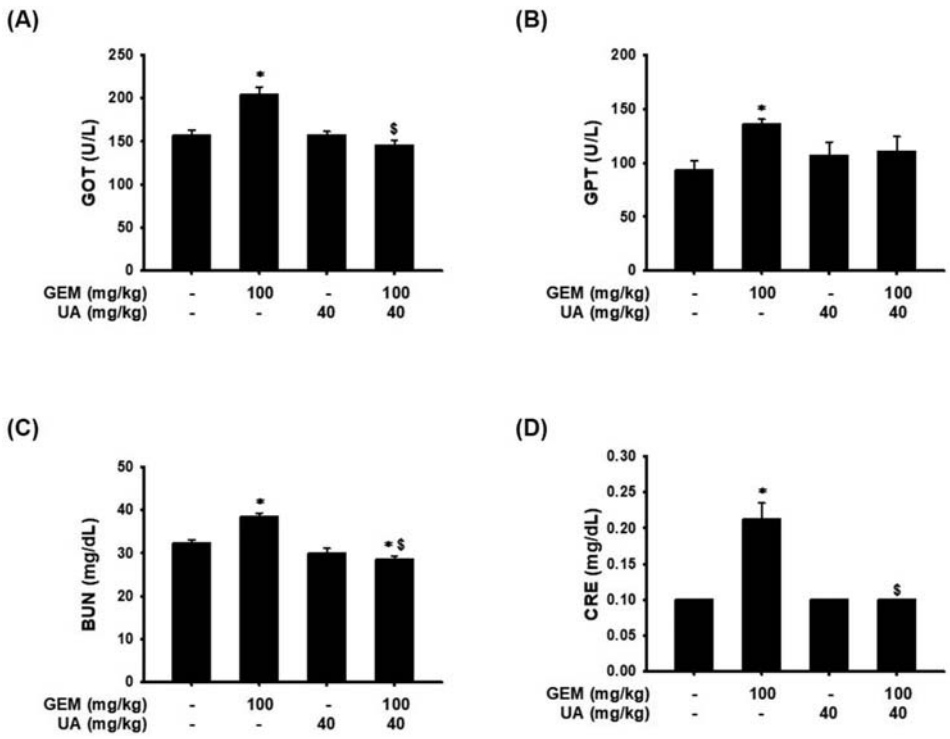


*Fig. 7. A decrease in GEM-induced liver injury and hepatotoxicity by UA administration in vivo. Treatment with GEM coupled with or without UA in MIA PaCa-2 $^{GEMR}$-bearing xenograft mice. Blood samples were collected for analysis of (A) GOT, (B) GPT, (C) BUN, and (D) creatinine. Data are presented as the mean ± S.E.M. (n = 8). *p < 0.05 vs. Control group and $^{\$}p < 0.05$ vs. GEM group.*

## 4. Discussions

GEM is the standard chemotherapeutic drug for pancreatic cancer treatment, yet nearly all patients either fail to react to GEM or rapidly develop chemoresistance. Articles merely mention that the metabolic clearance of GEM is a key factor for the development of chemoresistance, which may affect the capacity of second-line drug delivery and could salvage chemotherapy efficacy [34]. Thus, we herein explored whether UA was able to modulate drug efflux pump expression and enhance GEM efficacy. Our results revealed that GEM chemosensitivity was promoted upon UA incubation with pancreatic cancer cells. In particular, the RAGE/NF-κB/MDR1 axis was upregulated in GEM-resistant cells but was downregulated by UA administration. In addition to *in vitro* experiments, a xenograft mouse model also showed that UA combined with GEM exhibited an optimal result in limiting the size and volume of MIA PaCa-2 $^{GEMR}$ cell-bearing tumors. The coordinated changes in RAGE/NF-κB/MDR1 signaling protein expression *in vitro* and *in vivo* indicated that this combination strategy achieved the best tumor suppression effects in pancreatic cancer treatment.

Although previous studies found that NF-κB is a key regulator in pancreatic cancer chemoresistance, high levels of NF-κB are maintained by RAGE [29, 35]. However, the role of RAGE in the chemoresistance of pancreatic cancer is still unclear. Besides, UA has been found to inhibit pancreatic tumor growth and enhance GEM efficacy in a mouse model through repression of the inflammatory tumor microenvironment [36]. Nevertheless, there has been little evidence to support that the GEM efflux transporter is directly targeted by UA treatment. Our recent report revealed the underlying mechanisms of cell proliferation suppression and chemosensitivity enhancement by UA treatment [30]. The results showed that UA induces cell cycle arrest and endoplasmic reticulum (ER) stress, consequently causing apoptosis and autophagy by inhibiting the expression of RAGE in both GEM-sensitive and GEM-resistant MIA PaCa-2 cells [30]. In addition, our previous evidence showed that cell death and chemosensitivity are facilitated by quercetin treatment through suppression of RAGE initiated PI3K/AKT/mTOR/NF-κB axis in human pancreatic cancer cells [22], suggesting that development of GEM-resistance dependents on RAGE/NF-κB associated cascade via various signaling transductions. Furthermore, our previous study has shown that cytotoxicity (apoptosis and autophagy) enhancing effects induced by UA combined with

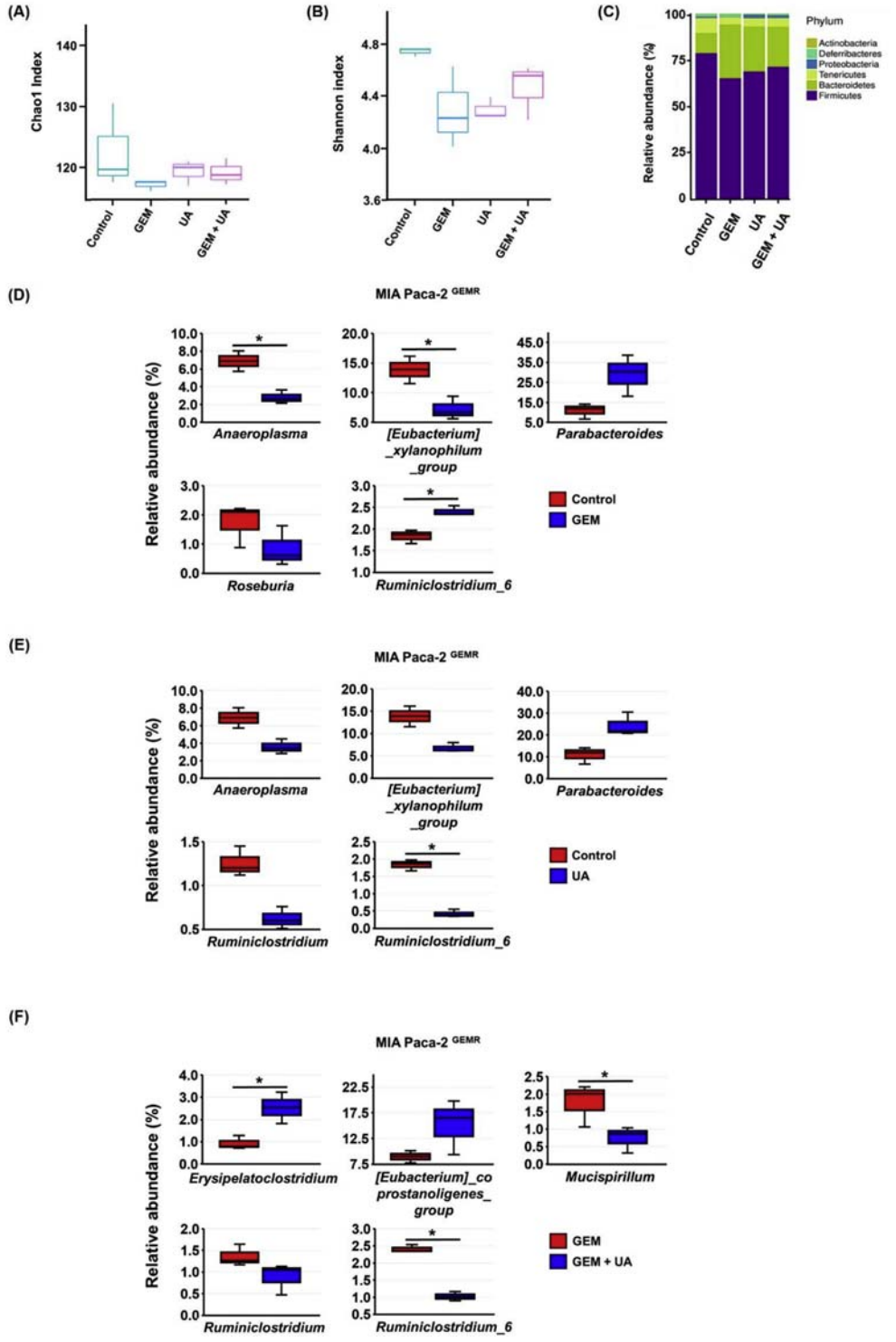


*Fig. 8. Manipulation of microbiota composition by UA administration in MIA PaCa-2 $^{GEMR}$-bearing xenograft mice. Treatment of MIA PaCa-2 $^{GEMR}$-bearing xenograft mice with GEM by itself or coupled with UA. Mouse fecal specimens were collected for microbiota analysis. (A) Chao1 was used for species richness estimation. (B) Shannon index was used for overall diversity measurement (richness and evenness). (C) Phylum level. The relative abundance of the dominant microbial strains in the (D) Control group vs. GEM group, (E) Control group vs. UA group, and (F) GEM group vs. GEM + UA group. ($n = 3$, $^*p < 0.05$).*

GEM treatment in both MIA Paca-2 and MIA Paca-2 $^{GEMR}$ cells [30]. Here, we found that the RAGE/NF-κB/MDR1 signaling axis was critical for GEM resistance and that it directly prohibited the MDR1 efflux transporter following UA treatment in GEM-resistant pancreatic cancer cells and in a MIA PaCa-2 $^{GEMR}$-bearing xenograft mouse model. To the best of our knowledge, this is the first report showing unique GEM-resistant signaling in pancreatic cancer and that it could be blocked by UA treatment both *in vitro* and *in vivo*.

GEM resistance is closely related to immune tolerance and leads to a poor survival rate in pancreatic cancer patients [37]. A report has found that GEM resistance is modulated by intratumor *Gammaproteobacteria* and its secreted long isoform of cytidine deaminase ($CDD_L$) enzyme [38]. However, the change in gut microbiota composition between cancer growth and immune response are complicated and unpredictable [39]. Previous evidence indicated that depletion of the gut microbiome does not reduce pancreatic tumor growth in recombination activating gene 1 (Rag1)-knockout immunodeficient mice, indicating that tumor immunity is an important process influenced by the gut microbiota [40]. Nevertheless, few studies have investigated the relationships between cancer-associated gut microbiota and immune-associated chemotherapy resistance. Recent reports have shown that the relative abundance of *Ruminiclostridium 6* and activation of the NF-κB pathway are significantly increased in dextran sulfate sodium (DSS)-induced ulcerative colitis BALB/c mice, implying that *Ruminiclostridium 6* may play a central role in regulating NF-κB activation [41, 42]. Moreover, the clinical trial found that higher relative abundance of *Ruminiclostridium* in children patients with acute lymphoblastic leukemia than in healthy controls [43]. In addition, the abundance of *Ruminiclostridium 6* is significantly lower in healthy volunteers compared to brain cancer patients [44], indicating that *Ruminiclostridium 6* may also involve in the growth of tumors. Interestingly, our results demonstrated that the relative abundance of *Ruminiclostridium 6* was substantially decreased in the UA and UA + GEM administration groups, and it was associated with NF-κB downregulation and tumor suppression.

Besides, UA has low dissolution and low oral bioavailability properties. Therefore, to explore the efficacy of UA by IP injection. Until now, it remains a limitation of calculating the metabolism of UA after IP injection in mice. However, a previous report found that IP injection of UA has a synergistic effect with oxaliplatin in suppressing NF-κB pathway and tumor growth in a xenograft mouse model of colorectal cancer [10]. In addition, our results represented compelling evidence that UA reduced the GEM resistance and tumor growth by IP injection. The above studies support that UA administration by IP injection is an appropriate method for chemosensitivity enhancement.

Although UA administration by IP injection effectively reduced tumor volume through gut microbiota modulation in pancreatic cancer xenograft mice model. However, a knowledge gap regarding the relationship between drug IP injection and gut microbiota modulation remains existence. Previous evidence showed that the intestinal microbiome accelerates pancreatic carcinogenesis in a subcutaneous xenograft Nod-SCID mice model, indicating microbiome can affect pancreatic carcinogenesis through long-distance connectivity that is independent of pancreatic microbiota and the pancreatic stromal microenvironment [45]. The consistent evidence suggested that a higher relative abundance of *Ruminiclostridium 6* was induced by IP administration of UA and consequently enhancement of chemosensitivity.

Notably, it has been shown that GEM induces liver injury and hepatotoxicity with elevations of AST and/or ALT levels in 30% to 70% [46-48]. More importantly, GEM-associated renal dysfunction and hemolytic uraemic syndrome have been demonstrated in pancreatic adenocarcinoma patients [49-51]. Consistently, our results recapitulated the clinical findings and found that GEM induced liver toxicity and kidney injury by significantly increasing GOT, GPT, BUN, and creatinine levels in laboratory mice. Strikingly, UA administration significantly improved hepatotoxicity and nephrotoxicity by reducing the crucial indicators of GOT, BUN, and creatinine levels in MIA PaCa-2 $^{GEMR}$ cell-bearing xenograft mice.

Overall, the compelling results herein demonstrated that UA significantly inhibits RAGE and NF-κB protein expression, subsequently attenuating the downstream MDR1 transporter and enhancing GEM chemosensitivity *in vitro*. Likewise, compelling evidence was collected in RAGE gene-silenced MIA PaCa-2 $^{GEMR}$ cells. Remarkably, an obstacle to tumor growth is found in mice administered UA and UA + GEM through the suppression of the RAGE/NF-κB/MDR1 axis. In addition, UA administration significantly impairs GEM-induced liver and kidney injury and modulates gut microbiota compositions, which is a novel finding. This is the first report showing that the GEM efflux transporter is directly targeted by UA both *in vitro* and *in vivo*, indicating that using UA as part of a combined strategy achieves the best tumor suppression effects in pancreatic cancer treatment.

## Conflict of interest

The authors declare no conflict of interests.

## Acknowledgements

This research work was supported in part by the grant MOST 109-2320-B-005-009- from the Ministry of Science and Technology, Taiwan.

## Reference

[1] Stoffel EM, McKernin SE, Brand R, Canto M, Goggins M, Moravek C, et al. Evaluating susceptibility to pancreatic cancer: ASCO provisional clinical opinion. J Clin Oncol 2019; 37:153−64.
[2] Siegel RL, Miller KD, Jemal A. Cancer statistics, 2020. CA Cancer J Clin 2020;70:7−30.
[3] Neoptolemos JP, Kleeff J, Michl P, Costello E, Greenhalf W, Palmer DH. Therapeutic developments in pancreatic cancer: current and future perspectives. Nat Rev Gastroenterol Hepatol 2018;15:333−48.
[4] Wolfgang CL, Herman JM, Laheru DA, Klein AP, Erdek MA, Fishman EK, et al. Recent progress in pancreatic cancer. CA Cancer J Clin 2013;63:318−48.
[5] Rahib L, Smith BD, Aizenberg R, Rosenzweig AB, Fleshman JM, Matrisian LM. Projecting cancer incidence and deaths to 2030: the unexpected burden of thyroid, liver, and pancreas cancers in the United States. Cancer Res 2014;74: 2913−21.
[6] Cargnin ST, Gnoatto SB. Ursolic acid from apple pomace and traditional plants: a valuable triterpenoid with functional properties. Food Chem 2017;220:477−89.
[7] Zhang N, Liu S, Shi S, Chen Y, Xu F, Wei X, et al. Solubilization and delivery of ursolic-acid for modulating tumor microenvironment and regulatory T cell activities in cancer immunotherapy. J Control Release 2020;320:168−78.
[8] Yin R, Li T, Tian JX, Xi P, Liu RH. Ursolic acid, a potential anticancer compound for breast cancer therapy. Crit Rev Food Sci Nutr 2018;58:568−74.
[9] Wang C, Shu L, Zhang C, Li W, Wu R, Guo Y, et al. Histone methyltransferase setd7 regulates Nrf2 signaling pathway by phenethyl isothiocyanate and ursolic acid in human prostate cancer cells. Mol Nutr Food Res 2018;62:e1700840.
[10] Shan J, Xuan Y, Zhang Q, Zhu C, Liu Z, Zhang S. Ursolic acid synergistically enhances the therapeutic effects of oxaliplatin in colorectal cancer. Protein Cell 2016;7:571−85.
[11] Jiang K, Chi T, Li T, Zheng G, Fan L, Liu Y, et al. A smart pH-responsive nano-carrier as a drug delivery system for the targeted delivery of ursolic acid: suppresses cancer growth and metastasis by modulating P53/MMP-9/PTEN/CD44 mediated multiple signaling pathways. Nanoscale 2017;9: 9428−39.
[12] Geerlofs L, He Z, Xiao S, Xiao ZC. Repeated dose (90 days) oral toxicity study of ursolic acid in Han-Wistar rats. Toxicol Rep 2020;7:610−23.
[13] Qiu J, Yang G, Feng M, Zheng S, Cao Z, You L, et al. Extracellular vesicles as mediators of the progression and chemoresistance of pancreatic cancer and their potential clinical applications. Mol Cancer 2018;17:2.
[14] Amrutkar M, Gladhaug IP. Pancreatic cancer chemoresistance to gemcitabine. Cancers (Basel) 2017;9:157.
[15] Hung SW, Mody HR, Govindarajan R. Overcoming nucleoside analog chemoresistance of pancreatic cancer: a therapeutic challenge. Cancer Lett 2012;320:138−49.
[16] Shahab U, Ahmad MK, Mahdi AA, Waseem M, Arif B, Moinuddin Ahmad S. The receptor for advanced glycation end products: a fuel to pancreatic cancer. Semin Cancer Biol 2018;49:37−43.
[17] Kang R, Tang D, Livesey KM, Schapiro NE, Lotze MT, Zeh 3rd HJ. The receptor for advanced glycation end-products (RAGE) protects pancreatic tumor cells against oxidative injury. Antioxid Redox Signal 2011;15:2175−84.
[18] Kang R, Hou W, Zhang Q, Chen R, Lee YJ, Bartlett DL, et al. RAGE is essential for oncogenic KRAS-mediated hypoxic signaling in pancreatic cancer. Cell Death Dis 2014;5:e1480.
[19] Wang H, Zhan M, Xu SW, Chen W, Long MM, Shi YH, et al. miR-218-5p restores sensitivity to gemcitabine through PRKCE/MDR1 axis in gallbladder cancer. Cell Death Dis 2017;8:e2770.
[20] Bergman AM, Pinedo HM, Talianidis I, Veerman G, Loves WJ, van der Wilt CL, et al. Increased sensitivity to gemcitabine of P-glycoprotein and multidrug resistance-associated protein-overexpressing human cancer cell lines. Br J Cancer 2003;88:1963−70.
[21] Huang CY, Chiang SF, Chen WT, Ke TW, Chen TW, You YS, et al. HMGB1 promotes ERK-mediated mitochondrial Drp1 phosphorylation for chemoresistance through RAGE in colorectal cancer. Cell Death Dis 2018;9:1004.
[22] Lan CY, Chen SY, Kuo CW, Lu CC, Yen GC. Quercetin facilitates cell death and chemosensitivity through RAGE/PI3K/AKT/mTOR axis in human pancreatic cancer cells. J Food Drug Anal 2019;27:887−96.
[23] Thomas RM, Jobin C. Microbiota in pancreatic health and disease: the next frontier in microbiome research. Nat Rev Gastroenterol Hepatol 2020;17:53−64.
[24] Pushalkar S, Hundeyin M, Daley D, Zambirinis CP, Kurz E, Mishra A, et al. The pancreatic cancer microbiome promotes oncogenesis by induction of innate and adaptive immune suppression. Cancer Discov 2018;8:403−16.
[25] Yu C, Chen S, Guo Y, Sun C. Oncogenic TRIM31 confers gemcitabine resistance in pancreatic cancer via activating the NF-kappaB signaling pathway. Theranostics 2018;8: 3224−36.
[26] Kimura K, Sawada T, Komatsu M, Inoue M, Muguruma K, Nishihara T, et al. Antitumor effect of trastuzumab for pancreatic cancer with high HER-2 expression and enhancement of effect by combined therapy with gemcitabine. Clin Cancer Res 2006;12:4925−32.
[27] Shanmugam MK, Rajendran P, Li F, Nema T, Vali S, Abbasi T, et al. Ursolic acid inhibits multiple cell survival pathways leading to suppression of growth of prostate cancer xenograft in nude mice. J Mol Med (Berl) 2011;89: 713−27.
[28] Hsu HY, Yang JJ, Lin CC. Effects of oleanolic acid and ursolic acid on inhibiting tumor growth and enhancing the recovery of hematopoietic system postirradiation in mice. Cancer Lett 1997;111:7−13.
[29] Li Q, Yang G, Feng M, Zheng S, Cao Z, Qiu J, et al. NF-kappaB in pancreatic cancer: its key role in chemoresistance. Cancer Lett 2018;421:127−34.
[30] Lin JH, Chen SY, Lu CC, Lin JA, Yen GC. Ursolic acid promotes apoptosis, autophagy, and chemosensitivity in gemcitabine-resistant human pancreatic cancer cells. Phytother Res 2020;34:2053−66.
[31] Lu CC, Huang BR, Liao PJ, Yen GC. Ursolic acid triggers nonprogrammed death (necrosis) in human glioblastoma multiforme DBTRG-05MG cells through MPT pore opening and ATP decline. Mol Nutr Food Res 2014;58:2146−56.
[32] Yeh CT, Wu CH, Yen GC. Ursolic acid, a naturally occurring triterpenoid, suppresses migration and invasion of human breast cancer cells by modulating c-Jun N-terminal kinase, Akt and mammalian target of rapamycin signaling. Mol Nutr Food Res 2010;54:1285−95.
[33] Shyu MH, Kao TC, Yen GC. Oleanolic acid and ursolic acid induce apoptosis in HuH7 human hepatocellular carcinoma cells through a mitochondrial-dependent pathway and downregulation of XIAP. J Agric Food Chem 2010;58:6110−8.
[34] Binenbaum Y, Na'ara S, Gil Z. Gemcitabine resistance in pancreatic ductal adenocarcinoma. Drug Resist Updat 2015; 23:55−68.

[35] Azizan N, Suter MA, Liu Y, Logsdon CD. RAGE maintains high levels of NFkappaB and oncogenic Kras activity in pancreatic cancer. Biochem Biophys Res Commun 2017;493: 592–7.
[36] Prasad S, Yadav VR, Sung B, Gupta SC, Tyagi AK, Aggarwal BB. Ursolic acid inhibits the growth of human pancreatic cancer and enhances the antitumor potential of gemcitabine in an orthotopic mouse model through suppression of the inflammatory microenvironment. Oncotarget 2016;7:13182–96.
[37] Delitto D, Perez C, Han S, Gonzalo DH, Pham K, Knowlton AE, et al. Downstream mediators of the intratumoral interferon response suppress antitumor immunity, induce gemcitabine resistance and associate with poor survival in human pancreatic cancer. Cancer Immunol Immunother 2015;64:1553–63.
[38] Geller LT, Barzily-Rokni M, Danino T, Jonas OH, Shental N, Nejman D, et al. Potential role of intratumor bacteria in mediating tumor resistance to the chemotherapeutic drug gemcitabine. Science 2017;357:1156–60.
[39] Goldszmid RS, Dzutsev A, Trinchieri G. Host immune response to infection and cancer: unexpected commonalities. Cell Host Microbe 2014;15:295–305.
[40] Sethi V, Kurtom S, Tarique M, Lavania S, Malchiodi Z, Hellmund L, et al. Gut microbiota promotes tumor growth in mice by modulating immune response. Gastroenterology 2018;155:33–37 e6.
[41] Li P, Wu M, Xiong W, Li J, An Y, Ren J, et al. Saikosaponin-d ameliorates dextran sulfate sodium-induced colitis by suppressing NF-kappaB activation and modulating the gut microbiota in mice. Int Immunopharmacol 2020;81:106288.
[42] Wu M, Li P, An Y, Ren J, Yan D, Cui J, et al. Phloretin ameliorates dextran sulfate sodium-induced ulcerative colitis in mice by regulating the gut microbiota. Pharmacol Res 2019;150:104489.
[43] Gao X, Miao R, Zhu Y, Lin C, Yang X, Jia R, et al. A new insight into acute lymphoblastic leukemia in children: influences of changed intestinal microfloras. BMC Pediatr 2020;20:290.
[44] Yang J, Moon HE, Park HW, McDowell A, Shin TS, Jee YK, et al. Brain tumor diagnostic model and dietary effect based on extracellular vesicle microbiome data in serum. Exp Mol Med 2020;52:1602–13.
[45] Thomas RM, Gharaibeh RZ, Gauthier J, Beveridge M, Pope JL, Guijarro MV, et al. Intestinal microbiota enhances pancreatic carcinogenesis in preclinical models. Carcinogenesis 2018;39:1068–78.
[46] Vincenzi B, Armento G, Spalato Ceruso M, Catania G, Leakos M, Santini D, et al. Drug-induced hepatotoxicity in cancer patients - implication for treatment. Expert Opin Drug Saf 2016;15:1219–38.
[47] Hailan WAQ, Abou-Tarboush FM, Al-Anazi KM, Ahmad A, Qasem A, Farah MA. Gemcitabine induced cytotoxicity, DNA damage and hepatic injury in laboratory mice. Drug Chem Toxicol 2020;43:158–64.
[48] Azad A, Chang P, Devuni D, Bichoupan K, Kesar V, Branch AD, et al. Real World Experience of Drug Induced Liver Injury in Patients Undergoing Chemotherapy. J Clin Gastroenterol Hepatol 2018;2:18.
[49] Walter RB, Joerger M, Pestalozzi BC. Gemcitabine-associated hemolytic-uremic syndrome. Am J Kidney Dis 2002;40:E16.
[50] Sahni V, Choudhury D, Ahmed Z. Chemotherapy-associated renal dysfunction. Nat Rev Nephrol 2009;5:450–62.
[51] Das A, Dean A, Clay T. Gemcitabine-induced haemolytic uraemic syndrome in pancreatic adenocarcinoma. BMJ Case Rep 2019;12:e228363.